Building a Driving Simulator with Parallax Barrier Displays

Christoph Schinko[1], Markus Peer[2], Daniel Hammer[2], Matthias Pirstinger[2], Cornelia Lex[2], Ioana Koglbauer[2], Arno Eichberger[2], Jürgen Holzinger[3], Eva Eggeling[1], Dieter W. Fellner[1] and Torsten Ullrich[1]

[1]*Fraunhofer Austria Research GmbH / Institut für ComputerGraphik & Wissensvisualisierung, TU Graz, Graz, Austria*

[2]*Institut für Fahrzeugtechnik, TU Graz, Graz, Austria*

[3]*AVL List GmbH, Graz, Austria*

Keywords: Driving Simulator, Parallax Barrier, Optimization.

Abstract: In this paper, we present an optimized 3D stereoscopic display based on parallax barriers for a driving simulator. The overall purpose of the simulator is to enable user studies in a reproducible environment under controlled conditions to test and evaluate advanced driver assistance systems.

Our contribution and the focus of this article is a visualization based on parallax barriers with (I) a-priori optimized barrier patterns and (II) an iterative calibration algorithm to further reduce visualization errors introduced by production inaccuracies. The result is an optimized 3D stereoscopic display perfectly integrated into its environment such that a single user in the simulator environment sees a stereoscopic image without having to wear specialized eye-wear.

1 INTRODUCTION

A parallax barrier is a device placed in front of a display enabling it to show stereoscopic, or multiscopic images without the need for the viewer to wear 3D glasses. Multiscopy differs from stereoscopy in that it displays multiple angles at once, allowing a viewer to see the content from different angles – not just a left-eye / right-eye angle. The parallax barrier consists of a material with a set of precision slits, or a translucent material with an opaque pattern, allowing each eye to see a different set of pixels. With this separation of the pixels it is possible to create an autostereoscopic display – a display without the need for glasses. This effect is illustrated in Figure 1.

The intended purpose for the parallax barrier technology in this context is an autostereoscopic display system for a driving simulator. It consists of a modified MINI Countryman chassis with eight liquid-crystal displays (LCDs) mounted around windscreen and front side windows. Four 55inch LCDs are placed radially around the hood of the car in a slanted angle. Two 23inch LCDs are used for each of the two front side windows. The four LCDs in the front are equipped with parallax barriers made of 2cm thick acrylic glass to minimize strain caused by the slanted angle. Each barrier is printed with a custom-made striped pattern, which is the result of an optimization process. The displays are connected to a cluster of four "standard" computers with powerful graphics cards. In order to account for movement of the driver's head inside the car, an eye-tracking system from SmartEye consisting of two cameras with infrared flashes is installed on the dashboard of the car. The position-depended rendering of the simulation scenario is performed on a cluster using the InstantReality framework.

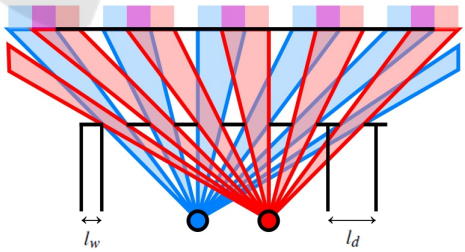

Figure 1: An autostereoscopic display can be realized using a parallax barrier. The barrier is located between the eyes (visualized in blue and red) and the pixel array of the display. It blocks certain pixels for each eye, which results in the eyes seeing only disjoint pixel columns (at least in an optimal setting). If the display is fed with correct image data, the user sees a stereo image. The free parameters (to optimize) are its line distance l_d and its line width l_w.

Schinko, C., Peer, M., Hammer, D., Pirstinger, M., Lex, C., Koglbauer, I., Eichberger, A., Holzinger, J., Eggeling, E., Fellner, D. and Ullrich, T.
Building a Driving Simulator with Parallax Barrier Displays.
DOI: 10.5220/0005711302810289
In *Proceedings of the 11th Joint Conference on Computer Vision, Imaging and Computer Graphics Theory and Applications (VISIGRAPP 2016) - Volume 1: GRAPP*, pages 283-291
ISBN: 978-989-758-175-5

2 RELATED WORK

2.1 Teaching, Learning, Testing in a Safe Environment

It is easy to understand why simulators have become such a critical tool for researchers and engineers in many fields of application. They not only constitute an excellent means of research for understanding human behavior, but also are an effective and cost-saving tool for designing human-machine-interaction interfaces (Eugen, 2008). Driving simulators for research and development are common today, for many reasons. The main advantages of simulators are (Pinto et al., 2008):

1. they provide the opportunity to study either rare or dangerous situations, as well as the environment and configurations that do not yet exist in the real world;
2. the parameters relevant to the conditions under study can be recorded and experimental setups can be strictly controlled;
3. they save time and money.

In the context of driving simulators, the applications range from research on emergency maneuvers (Malaterre, 1995), driving in fog (Cavallo and Pinto, 2001), and driver vigilance (Rogé et al., 2001) to driver training (Flexman and Stark, 1987), (Farmer et al., 1999), (Monin, 2004), dashboard design (Champion et al., 1999), road ergonomics (Hoekstra and van der Horst, 2000), and prototyping of lighting systems (Dubrovin et al., 2000).

2.2 3D Displays & Parallax Barrier

As already established in the introduction, a graphical display is autostereoscopic when all of the work of stereo separation is done by the display (Eichenlaub, 1998), so that the viewer does not need to wear special glasses.

Parallax barrier technology can be used to create autostereoscopic displays. While the technology is harder to apply for television sets, because of the requirement for a wider range of possible viewing angles, it is used in the Nintendo 3DS hand-held game console and in various smartphones (Benzie et al., 2007). Besides the use for 3D displays, the technology also allows to separate two views to use one display at the same time. These dual-view displays are, for example, used for the navigation system in the 2010-model Range Rover allowing driver and passenger to view different content.

Parallax barrier displays are quite simple to produce, but they have a number of limitations. The most important one is that they are limited to one user whose position needs to be fixed or is at least limited to a few viewing spots that depend on the viewing angle with respect to the display. In our scenario the limitation to a single user is not a problem, since it is limited to one user (the driver) anyway. The other part is the fact that the viewer must remain in a fixed position. This drawback can be eliminated by virtually adjusting the pixel columns such that the separation remains intact, as presented by (Sandin et al., 2001) and by (Peterka et al., 2007). In order to accurately adjust the pixels, some kind of user tracking is needed, which also limits the number of possible users. Most consumer products containing autostereoscopic displays, however, just combine parallax barriers with lenticular lenses. This approach does not put any constraints on the number of possible users at a time, but is relatively restricted concerning the possible viewing position(s).

Since the user's possible viewing positions are very limited in our scenario anyway, there is no need to adjust for large distance variations, for example, using a dynamic parallax barrier (Perlin et al., 2000). A static setup of the two cameras used by the eye-tracker is enough to cover the typical movement of a user.

Another drawback of the parallax barrier technique is that the resolution drops down to about a half for just a single user. In the presented scenario, this is not a critical point since the available resolution is sufficiently with respect to the distance of the driver (four displays each with a resolution of 1920×1080 pixels results in an overall resolution of more than eight megapixels).

Finally, the loss of brightness caused by the parallax barrier is a limitation for many use cases. Lanman et al. presented an approach for content-adaptive parallax barriers to overcome this issues by using an adaptive mask in a dual-stacked LCD (Lanman et al., 2010). However, the real-time application for dynamic content in a driving simulator is ruled out due to the involved computational complexity.

Glasses-free 3D Displays are not limited to use parallax barrier technology. Recent research by Wetzstein et al. provides alternatives to static parallax barrier solutions. One approach is based on a light field display using volumetric attenuators (Wetzstein et al., 2011). Another approach uses a family of compressive light field displays employing a stack of time-multiplexed, light-attenuating layers (Wetzstein et al., 2012).

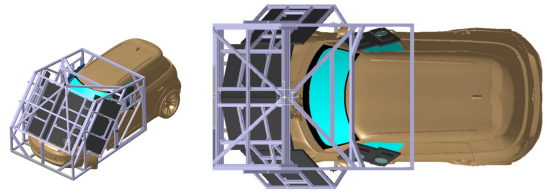

Figure 2: The result of the optimized display arrangement has been the basis of the simulator construction. This Figure illustrates the final setup with four 55" front displays and two 23" displays on each side.

3 PARALLAX BARRIER DISPLAY CONFIGURATION

During the design of the driving simulator, the display configuration has been optimized in a two step procedure (see Figure 2).

3.1 Display Arrangement

The first optimization step determines the best position of each display. The displays have to be arranged around a MINI Countryman, which is the basis of the driving simulator, without interfering or penetrating the vehicle's bodywork. Furthermore, the displays should obstruct the driver's view as much as possible in order to avoid distracting parts of the non-simulation environment being visible.

The optimization uses a cylindrical rendering as a cost function: the cameras are placed at the position of the driver's eyes, occluding geometry by the vehicle is supplied with a black / non-visible material, the displays are black / non-visible as well, and the whole scene is placed in surrounding, illuminating sphere in cyan and yellow – for each eye separately. The geometric setting is illustrated in Figure 3, while the result of the cost function of the optimal solution is shown in Figure 4. Each non-black pixel is a disturbing view past the displays. Minimizing the number of such pixels, improves the overall simulator experience.

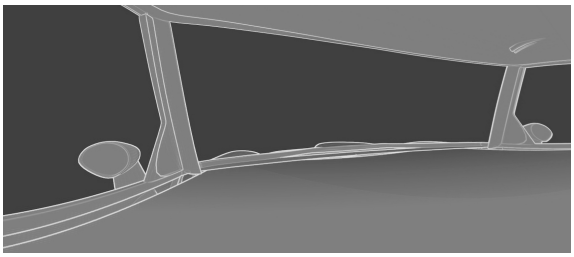

Figure 3: In order to optimize the display arrangement, the displays' visibility has been analyzed using cylindrical renderings from the driver's position.

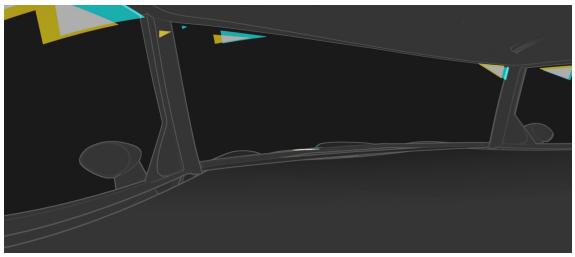

Figure 4: Using the setting illustrated in Figure 3 with occluding vehicle geometry and displays rendered in black, and the environment rendered in cyan and yellow for each eye separately, the cost function can be minimized easily: Each non-black pixel is a disturbing view past the displays. These pixels should be removed. For ease of understanding Figure 3 is overlaid semi-transparently.

3.2 Pattern Optimization

The first step of the optimization of the display configuration determined the best position of each display. The second step uses the display position and the driver's position in order to optimize the barrier pattern. In detail, the barrier pattern is a set of lines, which is printed on 2cm thick acrylic glass in the front of each display. The pattern is described by three parameters; i.e. the line width l_w, the distance between two consecutive lines l_d measured between medial axes, and their deviation from a vertical alignment l_a. The cost function of the second optimization routine depends on these three parameters. In each evaluation a geometric scene is generated (including the vehicle, the displays, and the line of the barrier pattern). For each scene, the rays – from the position of the driver's eyes to each display pixel – check the visibility of a display pixel for each eye.

The result for each pixel can be: (i) visible by both eyes, (ii) visible by left eye only, (iii) visible by right eye only, or (iv) not visible at all. The objective function simply counts the number of pixels, which can be seen by both eyes, or which cannot be seen at all (i.e. which are not separable). More details on this optimization process have been published in (Eggeling et al., 2013).

The optimization returns the optimal configuration. Unfortunately, the manufactured driving simulator differs significantly from its specification:

- As the displays and the barriers are arranged in an inclined plane, sagging effects in the order of millimeters occur.
- The printed parallax barrier pattern has not the required precision; that is, the lines are up to 0.15mm (+12.4%) wider than specified.
- The refractive index of the acrylic glass has not been considered in the planning stage.

While the first problem has been fixed with additional mountings, the second and the third problem have been solved via the calibration described below.

4 PARALLAX BARRIER DISPLAY CALIBRATION

Due to the already mentioned deviations of the manufactured acrylic glasses from the ideal ones, additional calibration steps became necessary. We opted for a calibration solution on-site because of possible inaccuracies in the direct measurement of display and parallax barrier parameters, and the inability to make exact measurements of the distance from the display's pixel array to the parallax barrier – at least without disassembling the displays. Also we need to take influences of the environment, like lighting conditions and heat development of all participating components, into account.

To establish a ground truth, we need accurate measurements of a number of display and barrier parameters. Some parameters are scalar values (e.g. distance between two consecutive lines of a parallax barrier l_d), while others are vectors (e.g. the global position of the parallax barriers and the displays) that need to be registered to a global coordinate system. A first idea to measure vector-valued parameters using a robotic arm was soon discarded due to the intricate construction of the mounting frame for the displays and the resulting inaccessibility of the corner points. A second idea to use a tracked (using the eye-tracker) laser distance measuring unit was discarded as well due to line of sight problems.

The solution we opted for is an indirect system using a digital video camera. Since we already have initial values from direct measurements and the digital construction of the driving simulator, we can optimize the parameters by evaluating a video feed from a camera. In this way, we do not optimize and calibrate the display parameters directly, but we calibrate the end result.

This calibration is done for each display separately. It requires a custom mounting for the camera to be able to account for horizontal rotation. Therefore, the optical center of the camera was measured using a Panosaurus device from Gregwired. Afterwards we created a matching mounting to be able to rotate the camera horizontally around it's center (initial tests revealed that no vertical rotation is necessary). Attaching the mount in the driving simulator was no difficult task, since we already had a mounting for the calibration pattern of the eye-tracking system. We modified it for the camera mount to be placed exactly in the position of left and right eye (separated by 65mm).

Our parallax barrier display calibration consists of several steps that are designed to be performed one after the other.

4.1 Video Mask Determination

In a first step, we render two images and capture them with the video feedback loop. One image is completely black; the other one is completely white (see Figure 5, left). We perform this step in order to automatically create a mask, which is used in all subsequent steps to restrict the calibration to the display's area and to ignore irrelevant parts of the video images. For each pixel the mask stores a value between zero and one indicating whether the pixel shows a part of the display (1.0) or not (0.0 otherwise). The result is shown in Figure 5, right.

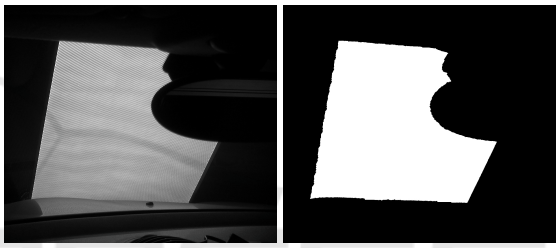

Figure 5: The parallax barrier display calibration only uses clipped / weighted video input. The corresponding mask is generated in the first step. Although the automatically generated mask is sufficient, we advise to use a manually clipped mask as shown on the right hand side. (The occluder in the upper right part of the images is the MINI's interior mirror).

4.2 Color Calibration

The next step is to perform a single color test to compare input colors (sent to a display) with output colors (captured by the video camera) for a configurable amount of colors (256 per default) spread evenly in the RGB color space. A smaller example is shown in Figure 6. This step is done in order to take color deviation into account. Color deviation occurs due to non-calibrated hardware and due to color shifting effects caused by looking at the displays at an angle. The error function of the color calibration is the sum of per-pixel differences weighted with the normalized mask of the previous step.

4.3 Display Calibration

The third and the fourth steps are the optimization of the barrier parameters: we start in the third step with the sampling of the parameter space using the theoretical parameters (the values the parameters should

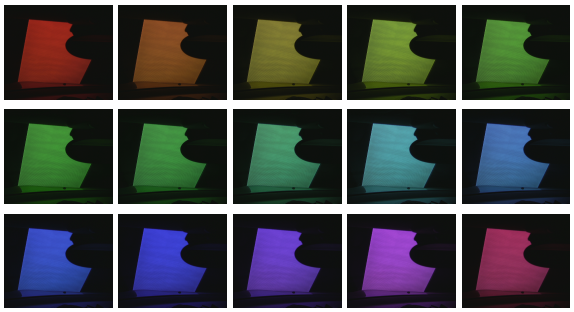

Figure 6: The color calibration step is performed to reduce hardware-based color shifting effects. These 15 images show the captured results of fully saturated colors with varying hue. In our setting the color red shows exceedingly few shifting effects. Consequently, it is the selected color for the following calibration steps.

have according to the construction plan) extended to a sufficiently large interval. The fourth step uses the best configuration of the third step and performs a fine-tuning using a minimizing optimization routine.

In both steps we use the following setup. We start with a parameter vector, i.e., the assignment of all variables (barrier line width l_w, barrier line orientation l_α, barrier line vertical offset l_y, etc.). Based on these values, a test image is calculated. It shows a black pixel, if the pixel is visible from the eye position at which the camera is currently positioned. Otherwise a colored pixel (using the color determined in the color calibration step) is shown. Having calculated the test image, our calibration tool displays the image and captures the video image to check the result. The goal is to have a completely black image. Consequently, the error function simply counts the number of non-black pixels weighted with the calibration mask.

While the third step is a sampling of the multidimensional parameter space to obtain uniformly distributed samples (see Figure 7, left), the fourth step uses the same error function and the best sample in order to fine-tune the settings with a conjugate direction search routine (see Figure 7, right).

During several calibrations we made some interesting observations:

- The parameters *barrier line width* l_w and *barrier line distance* l_d are not independent (see Figure 1). If the optimization routine does not have additional constraints, it returns a parameter setting, which corresponds to a black test image and therefore in a black video captured image. We solved this problem by introducing the linear constraint $2 \cdot l_w = l_d$, which we identified heuristically in a manual optimization test.
- The optimization routine returns the same configuration for both eyes (with the numerical precision of the termination condition used by the optimization routine), although the calibrations have been performed separately. Therefore, we have not been confronted with the problem of handling two different parameter settings and how to merge / combine them.
- The complete calibration is not optimized for speed, but it runs completely automatically and can be started at any step, if previous results are available. In practice, the color calibration is performed once, for one eye position only. Also it is also possible to directly define a staring set of parallax barrier parameters to skip the time consuming sampling step in the second stage and directly start with the optimization routine.

4.4 Parameter Tuning

With the optimized set of parameters at hand, the first tests with real persons using the eye-tracking data revealed problems with ghosting effects, thus the pixel separation was not ideal. Having ruled out any problems in the visualization pipeline, we encountered two problems.

1. The size of a pixel with respect to the line width of the barrier is rather large. Depending on the viewing angle, it is possible to have a pixel classified as visible by one eye, while nearly half of the pixel is visible for both eyes.
2. We also found the eye-tracking data to be the source of inaccuracy – the two camera system is struggling with partial occlusion and/or bad lighting conditions.

A solution to overcome these issues is to virtually increase the parameter value of the barrier line width.

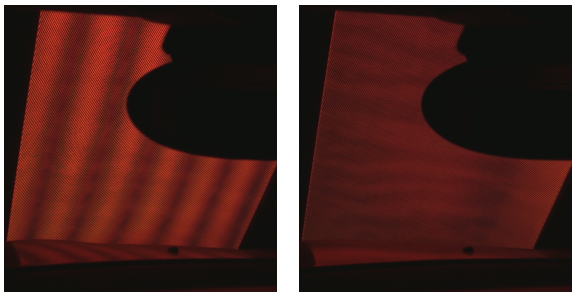

Figure 7: The display calibration optimizes the parameter configuration using a sampling of the multidimensional parameter space to obtain uniformly distributed samples and a directed conjugate search routine. On the left hand side the Figure shows a bad configuration captured during the sampling stage. The right hand side shows a good, final configuration.

This way the virtual barrier becomes larger and more pixels are considered as non-separable. They are visible by both eyes or not visible at all. This solution reduces ghosting at the cost of resolution and brightness (as non-separable pixels are rendered black). The reduced resolution was observable in driving scenarios with detailed models and textures. We did not encounter any problems concerning brightness, because the environment in the driving simulator is very dark.

4.5 Runtime

Visualizing a scene in the driving simulator is handled by the InstantReality framework. Several components work hand in hand to incorporate user tracking as well as autostereoscopic rendering. User tracking is carried out by a SmartEye eye-tracking system with two cameras mounted at the base of the A-pillar on the dashboard and inside the left ventilation vent of the co-driver. This placement ensures minimal occlusion caused by the steering wheel and the necessary degree of inconspicuousness for drivers to not feel observed. The mandatory infrared flashes however are clearly visible (see Teaser Figure). The eye-tracking system provides head position and rotation as well as the position of left and right eye. These values are needed to calculate the correct perspective projection and to take the parallax barrier into account using a custom InstantReality node.

In detail, the perspective projection is directly handled by the InstantReality framework, while all parallax barrier calculations are performed using a multi-pass shader pipeline. In a first step, the images for left and right eye are rendered off-screen into two textures. A fragment shader in the following pass performs intersection tests (viewing ray $\leftrightarrow$ parallax barrier) at runtime from both eyes to all display pixels for the classification of the pixels (visible by both eyes, visible by left eye only, visible by right eye only, not visible). With the classification of the pixels at hand, the corresponding values from the textures are used to create the final image. Pixels visible by both eyes as well as pixels not visible are set to black.

For the simulation part of the driving simulator, the visualization is a black box for visualizing a scene graph. All updates are sent using the External Authoring Interface of the InstantReality framework. The visualization system on the other hand is not dependent on the simulation.

5 EVALUATION

The complete optimization (including video mask determination, color calibration, display calibration, and parameter tuning) ran fully automatically and needed approximately $2\frac{1}{2}$ hours per display. The final barrier parameters returned by the calibration routine has led to an error of 14%–16%; i.e. approximately one-seventh of all pixels show a wrong color for at least one eye. These values have been used in a final user study with 21 test persons. Each test consisted of different, combined driving situations including inner city scenarios, overland tours and high-speed motorway driving. The participants answered several questions during the test phase and afterwards. The questionnaire consisted of the standardized simulator sickness questionnaire (Kennedy et al., 1993), general questions about the overall system and specific questions on relevant subsystems such as visualization, physical simulation, haptic realism of the force-feedback devices, acoustics, etc. In the following subsections we focus on the overall impression including simulator sickness and visualization specific aspects.

5.1 Visualization System

The visualization system has a large influence for the overall experience with the driving simulator. While some preliminary tests have been conducted using 2D visualization, the majority of the scenarios was tested in 3D. Since it is not easily possible to remove the parallax barriers, the participants had to deal with the parallax barriers during tests in 2D as well.

On a scale from *unrealistic* to *realistic*, 16 out of 21 participants (about 76%) evaluated the visualization system as being *rather realistic* or *realistic*. Three participants deemed the visualization system to be *unrealistic*. Two of them had problems with ghosting effects and projection offsets which are caused by problems of the eye-tracking system. The last participant of the three was not experiencing these effects, but suffered from general discomfort.

With the same scale, 13 out of 21 participants (about 62%) experienced the representation of the environment (i.e. the modeled 3D scene) as *rather realistic* or *realistic*. One of the participants voted with *unrealistic*. The participant was one of the three experiencing the visualization system as unrealistic.

From the 21 participants, 20 (about 95%) answered neutral or positive when asked to rate the driving simulator towards usefulness – 15 of them rated positive. The remaining participant was the one suffering from general discomfort.

A total of 14 participants (about 67%) would definitely partake in another study using this driving simulator; two participants would not. When asked to recommend the driving simulator to other drivers, 17

(about 81%) participants would do so. One participant answered *negative* when asked which impression of the driving simulator other drivers would get.

Answering open questions, one participant deemed the 3D visualization as being the most useful part of the driving simulator. On the other hand, participants had problems with dizziness, ghosting effects, the parallax barrier lines as well as stifling air. One participant struggling with ghosting effects had difficulties in perceiving speed with the 2D visualization, but had a better perception in 3D. We also had a suggestion to change the color of the parallax barrier lines from black to some color with less contrast. Regarding the choice of the preferred visualization, we had an almost neutral result between 2D and 3D.

5.2 Simulator Sickness Questionnaire

Simulator sickness and motion sickness result in feelings of nausea, dizziness, vertigo, and sweating (among other symptoms). Simulator sickness is generally the result of the discrepancy between simulated visual motion and the sense of movement stemming from the vestibular system (Balk et al., 2013). In many simulators, the visual system receives information that suggests movement (e.g., roadway scenes passing by the viewer), yet the vestibular system interprets a stationary status. It is this discrepancy that causes simulator sickness in many people.

There are many different ways to assess simulator sickness. The most popular way is the Simulator Sickness Questionnaire (SSQ) by R. S. Kennedy et al. (Kennedy et al., 1993). This questionnaire asks participants to score 16 symptoms (of three general categories: oculomotor, disorientation, and nausea) on a four point scale (0-3). Weights are assigned to each of the categories and summed together to obtain a single score.

The average values of our driving simulator using parallax barrier techniques in the categories oculomotor, disorientation, and nausea are listed in Table 1 (evaluated according to Fisher et al (Fisher et al., 2011)). The Table includes comparative values published by Häkkinen et al. (Häkkinen et al., 2006), who investigated "Simulator sickness in virtual display gaming: a comparison of stereoscopic and non-stereoscopic situations".

Table 1: The driving simulator using parallax barrier has been evaluated using the Simulator Sickness Questionnaire *(Kennedy et al., 1993)*. In order to interpret the scores we include comparative values for non-stereoscopic displays (Virtual 2D) and stereoscopic displays using shutter techniques (Virtual 3D) *(Häkkinen et al., 2006)*.

	Parallax Barrier	Virtual 2D	Virtual 3D
nausea	34.9	11.8	29.9
oculomotor	49.8	14.0	26.9
disorientation	79.5	21.1	41.1

6 CONCLUSION & FUTURE WORK

This article describes the construction, design, optimization, calibration and evaluation of a parallax barrier on a driving simulator.

6.1 Contribution

This work presents a real system by a selective examination of specific aspects embodied in the system. To the best of our knowledge, our driving simulator is the first one with parallax barrier stereoscopic displays.

While each single component has been investigated before (Eggeling et al., 2013), the combination and interaction of all parts has been a challenge. Therefore, the description of the lessons learned (see Section 3. and 4.) are a valuable contribution – especially, the approach to use a video feedback loop and the calibration routine to compensate for

- hardware inaccuracies and
- problems due to inaccessible displays, respectively intricate direct measurements.

6.2 Benefit

When faced with the question which visualization technique to be used in the context of a simulator environment, our evaluation gives decision support: it allows a reader to assess parallax barrier techniques. Some aspects (hardware costs, etc.) can be estimated in advance, while other ones (user acceptance, simulator sickness, etc.) cannot be estimated beforehand. Based on the "in advance estimation", we have chosen the parallax barrier technique mainly due to its reduced costs.

Concerning user acceptance, the evaluation uses the "standardized" Simulator Sickness Questionnaire (Kennedy et al., 1993) and relates the scores of the barrier approach with shutter-based, stereoscopic solutions. Unfortunately, the parallax barrier approach is still not the first choice considering simulator sickness.

6.3 Future Work

A question of future research is what to do with the pixels that are visible by both eyes. Preliminary tests using a blend of both images for these pixels resulted in significant ghosting effects. These effects are noticeable in areas of high frequency (i.e. with large differences in the pixel values of the two images), but are less noticeable in homogeneous regions. An idea would be to use the pixels only for these areas to obtain more overall brightness.

With the availability of the gaze direction provided by the eye-tracking system it is possible to restrict the parallax barrier calculation to a certain region. The idea is to have a two-dimensional rendering for peripheral areas and do intricate barrier calculations only in an area around the gaze direction. This kind of rendering may reduce the simulator sickness. An open question in this context is whether there is a need to predict the movement of the eye, or the update rate of the eye positions (totally depending on the eye-tracking system) is sufficiently high.

Especially in driving scenarios, dazzling effects play an important role; they are difficult to implement using standard display hardware because of low dynamic range of the light source. Such High Dynamic Range effects can be approximated using special rendering techniques – but only to a limited degree.

ACKNOWLEDGEMENT

This work is part of the project “MueGen Driving”, funded by the Austrian Ministry for Transport, Innovation and Technology and the Austrian Research Agency in the FEMtech Program *Talents*. Furthermore, it is supported by the government of the Austrian federal state of Styria within the project “CUBA – Contextual User Behavior Analysis”.

REFERENCES

Balk, S. A., Bertola, A., and Inman, V. W. (2013). Simulator Sickness Questionnaire: Twenty Years Later. *Proceedings of the International Driving Symposium on Human Factors in Driver Assessment, Training, and Vehicle Design*, 7:257–263.

Benzie, P., Watson, J., Surman, P., Rakkolainen, I., Hopf, K., Urey, H., Sainov, V., and von Kopylow, C. (2007). A Survey of 3DTV Displays: Techniques and Technologies. *IEEE Transactions on Circuits and Systems for Video Technology*, 17:1647–1658.

Cavallo, V. and Pinto, M. (2001). Does Speed Perception Indeed Fog up as Visibility Drops? *Proceedings of the International Conference Vision in Vehicles*, 9:308–314.

Champion, A., Mandiau, R., Kolski, C., Heidet, A., and Kemeny, A. (1999). Traffic Generation with the SCANER II Simulator: Towards a Multi-Agent Architecture. *Proceedings of Driving Simulation Conference*, 5:1–15.

Dubrovin, A., Lelevé, J., Prévost, A., Canry, M., Cherfan, S., Lecocq, P., Kelada, J. M., and Kemeny, A. (2000). Application of Real-Time Lighting Simulation for Intelligent Front-Lighting Studies. *Proceedings of Driving Simulation Conference*, 6:32–38.

Eggeling, E., Halm, A., Fellner, D. W., and Ullrich, T. (2013). Optimization of an Autostereoscopic Display for a Driving Simulator. *Joint Conference on Computer Vision, Imaging and Computer Graphics Theory and Applications*, 8:318–326.

Eichenlaub, J. B. (1998). Lightweight compact 2D/3D autostereoscopic LCD backlight for games, monitor, and notebook applications. *Stereoscopic Displays and Virtual Reality Systems*, 5:180–185.

Eugen, T. (2008). *Use and validation of driving simulators*. Doctoral Theses at NTNU (Norwegian University of Science and Technology).

Farmer, E., Reimersma, J., Moraal, J., Jorna, P., and Van Rooij, J. (1999). *Handbook of Simulator-Based Training*. Ashgate Publishing.

Fisher, D. L., Rizzo, M., and Caird, J. K. (2011). *Handbook of Driving Simulation for Engineering, Medicine, and Psychology*. Crc Press Inc.

Flexman, R. P. and Stark, E. A. (1987). Training simulators. *Handbook of Human Factors*, 1:1012–1037.

Häkkinen, J., Pölönen, M., Takatalo, J., and Nyman, G. (2006). Simulator sickness in virtual display gaming: a comparison of stereoscopic and non-stereoscopic situations. *Proceedings of the conference on Human-computer interaction with mobile devices and services*, 8:227–230.

Hoekstra, W. and van der Horst, A. R. A. (2000). New road designs tested in a driving simulator. *Proceedings of Driving Simulation Conference*, 6:1–6.

Kennedy, R. S., Lane, N. E., Berbaum, K. S., and Lilienthal, M. G. (1993). Simulator Sickness Questionnaire: An enhanced method for quantifying simulator sickness. *Journal of Aviation Psychology*, 07:203–220.

Lanman, D., Hirsch, M., Kim, Y., and Raskar, R. (2010). Content-adaptive Parallax Barriers: Optimizing Dual-layer 3D Displays Using Low-rank Light Field Factorization. *ACM Trans. Graph.*, 29(6):163:1–163:10.

Malaterre, G. (1995). Comparisons between simulation and actual driving situations: Some experiments. *Proceedings of Driving Simulation Conference*, 2:60–76.

Monin, C. (2004). TRUST3000: The truck simulator for advanced continuous professional training. *Proceedings of Driving Simulation Conference*, 8:389–399.

Perlin, K., Paxia, S., and Kollin, J. S. (2000). An Autostereoscopic Display. *Proceedings of the annual conference on Computer graphics and interactive techniques*, 27:319–326.

Peterka, T., Kooima, R. L., Girado, J. I., Ge, J., Sandin, D. J., and A., D. T. (2007). Evolution of the Varrier Autostereoscopic VR Display: 2001–2007. *Stereoscopic Displays and Virtual Reality Systems*, 14:1–11.

Pinto, M., Cavallo, V., and Ohlmann, T. (2008). The development of driving simulators: toward a multisensory solution. *Le travail humain*, 71:62–95.

Rogé, J., Pebayle, T., and Muzet, A. (2001). Variations of the level of vigilance and of behavioral activities during simulated automobile driving. *Accident Analysis and Prevention*, 33:181–186.

Sandin, D. J., Margolis, T., Dawe, G., Leigh, J., and A., D. T. (2001). The Varrier Auto-Stereographic Display. *Stereoscopic Displays and Virtual Reality Systems*, 8:1–8.

Wetzstein, G., Lanman, D., Hirsch, M., and Raskar, R. (2012). Tensor displays: Compressive light field synthesis using multilayer displays with directional backlighting. *ACM Trans. Graph.*, 31(4):1–11.

Wetzstein, G., Lanman, D., W., H., and R., R. (2011). Layered 3D: Tomographic image synthesis for attenuation-based light field and high dynamic range displays. *ACM Trans. Graph.*, 30(4):95:1–95:12.